https://doi.org/10.5194/egusphere-2025-6237
Preprint. Discussion started: 12 February 2026
© Author(s) 2026. CC BY 4.0 License.

Agricultural methane plume detection using MethaneAIR: A targeted scene-based approach with wavelet denoising and divergence integral methods.

Penelope Smale[1], Alexander Geddes[1], Sara Mikaloff-Fletcher[1], Zhan Zhang[3,4], Apisada Chulakadabba[3], MaryAnn Sargent[3], Steven Wofsy[3], Joseph Rudek[2], Jonathan Franklin[3], Jack Warren[4].

[1]Earth Sciences New Zealand, Private Bag 50061, Lauder, 9320, New Zealand
[2]Environmental Defense Fund, New York, NY, USA
[3]Harvard John A. Paulson School of Engineering and Applied Sciences, Harvard University, Cambridge, MA,
[4]Environmental Defense Fund, Washington, D.C., USA

Correspondence to: Penny Smale (penny.smale@niwa.co.nz)

Abstract. Methane is a potent greenhouse gas, and accurate emission estimates are essential for effective climate mitigation. Agricultural sources, particularly concentrated animal feeding operations (CAFOs), are significant anthropogenic contributors, yet their emissions remain difficult to quantify, contributing to uncertainty in inventories.

MethaneAIR, an aircraft-based imaging spectrometer and precursor to MethaneSAT, was primarily developed to characterize methane emissions from oil and gas infrastructure. Between 2021 and 2024, MethaneAIR conducted 75 flights across the United States and Canada, producing orthorectified mosaics of column-averaged methane. These data were used to assess agricultural emissions at high resolution through a novel scene-based approach. Agricultural "scenes" were defined as spatial subsets of flight mosaics encompassing CAFOs and surrounding areas, enabling targeted plume detection and quantification. Wavelet denoising and a Gaussian-based Divergence Integral method were applied to 209 agricultural scenes coincident with 84 CAFOs. Of 200 detected plumes, 89 met our quantitative robustness criteria and were analysed further, with emphasis on northeast Colorado.

While limited on-farm data, such as the number of animals and waste management practices, constrained the ability to fully interpret emission drivers, the analysis revealed elevated emissions relative to inventories and high variability, likely influenced by interactions between wind and waste management systems. These findings both highlight variability not captured in annual inventories and inform the design of future satellite missions like MethaneSAT, which will improve global methane monitoring and climate models. With improved on-farm information, this approach could provide a scalable pathway for emission and mitigation verification.

1 Introduction

Methane (CH_4) emission reductions are an effective method to mitigate near term climate change as CH_4 is both a potent greenhouse gas (GHG) and short lived (IPCC, 2023). Global atmospheric methane has increased substantially since pre-industrial values (Saunois et al., 2024) with a record high growth rate between 2020 and 2022 (Michel et al., 2024). Globally, agriculture is the largest anthropogenic methane source, at 40% (Saunois et

https://doi.org/10.5194/egusphere-2025-6237
Preprint. Discussion started: 12 February 2026
© Author(s) 2026. CC BY 4.0 License.

al., 2024). This is in turn dominated by emissions from livestock agriculture in the form of enteric fermentation and manure management.

Enteric fermentation is a natural digestive process in ruminant animals where anaerobic microbes (methanogens) break down feed, producing methane (CH_4) as a byproduct, released through burping. The quantity of CH_4 produced is dependent on animal species, animal life stage, diet composition, feed intake, and digestive efficiency (Roques et al., 2024).

Within manure management systems, open anaerobic lagoons are a particularly important source of methane emissions. These lagoons emit methane through microbial decomposition and are highly sensitive to environmental conditions such as wind and temperature, which can influence emission rates and plume detectability (Golston et al., 2020; Ouatahar et al., 2024). In the USA, 36% of anthropogenic methane emissions are attributed to agriculture (U.S. Environmental Protection Agency, 2024).

CH_4 emissions can be quantified using bottom-up (reported inventory) and top-down (atmospheric measurement) approaches. Inventories of agricultural methane emissions, used for tracking and reporting, are primarily based on an emission factor (EF) per animal (IPCC, 2006), which can be a default value or use more detailed country-specific information to account for different animals, feed types and management practices (IPCC, 2019). As part of the United States GHG reporting, the Environmental Protection Agency (EPA) Methane inventory applies regional, animal, and process specific EF's (IPCC's tier 3) including enteric fermentation and manure management and is made available in a gridded format on an annual basis. However, methane emissions can vary considerably temporally far beyond the mean, due to animal behaviour, management practices, diet, and environmental conditions(Tedeschi et al., 2022; Leytem et al., 2017; Mead et al., 2024; Golston et al., 2020). While emission inventories are adopting more sophisticated methods to estimate methane emission factors (Maasakkers et al., 2023; Mead et al., 2024), substantial uncertainties persist. This is exacerbated when considering individual farms and facilities.

Top-down measurements, where atmospheric methane concentrations are used to infer emission rates, have been widely applied at global to regional scales (e.g. Worden et al. (2022) and Jacob et al. (2022)) supporting the validation and refinement of emission inventories (Maasakkers et al., 2019). However, discrepancies between bottom-up and top-down approaches exist, with several reports of inventory underestimating regional and national emissions compared to top-down approaches (Jacob et al., 2016; Jacob et al., 2022; Saunois et al., 2024; Yu et al., 2021; Wójcik-Gront and Wnuk, 2025). Incongruities arise from multiple sources; for example, bottom-up approaches do not always account for all methane sources (National Academies of Sciences, 2018), while top-down do not generally have spatial and temporal resolutions to identify and quantify sources (Saunois et al., 2024), though this is changing with high resolution point source mappers.

At a facility level, top-down approaches have advanced significantly through the wide-spread use of techniques such as hyperspectral imaging enabling a shift to plume quantification (Varon et al., 2018; Li et al., 2024; Schuit et al., 2023). TROPOMI and GHGSat have been used to detect large methane plumes, including those from urban areas and landfills. Varon et al. (2018), using GHGSat-D, demonstrated that emissions as small as 0.03 t h^{-1} could

https://doi.org/10.5194/egusphere-2025-6237
Preprint. Discussion started: 12 February 2026
© Author(s) 2026. CC BY 4.0 License.

be detected under controlled conditions. Building on this, Sherwin et al. (2023) evaluated nine satellite platforms including GHGSat-C, PRISMA, EnMAP, WorldView-3, Sentinel-2, and Landsat 8 and confirmed that GHGSat-C was capable of detecting emissions down to 0.03 t h^{-1}, while other systems exhibited minimum detection thresholds ranging from approximately 0.2 to 7.2 t h^{-1}. Wind speed was identified as a key source of uncertainty in quantification (Sherwin et al., 2024). Li et al. (2024) used the Chinese GF5-01A/02 hyperspectral satellites to detect oil and gas plumes across in North America, with emission rates ranging from 0.52 to 16.07 t h^{-1}. Schuit (2023) notes that targeting known emission sites improves detection, and Li et al. (2024) similarly suggest that future surveys could benefit from more targeted assessments with additional data.

MethaneSAT, a combined American initiative led by the Environmental Defense Fund (EDF) and its subsidiary MethaneSAT LLC, together with Aotearoa New Zealand partners, was developed and launched in 2024 with the primary purpose to quantify Oil and Gas CH_4 emissions at better spatial and temporal resolution than existing satellite measurements (Chan Miller et al., 2024). The MethaneSAT has a native resolution of 100 x 400 m over targeted 200 km x 200 km regions of interest with precision of 2-3 ppb at 1.5 x 1.5 km resolution. This unique combination is ideal for wide scale monitoring of oil and gas emissions and other large point sources, such as intensive livestock operations, as well as diffuse agriculture. Although communication with MethaneSAT was lost in 2025, the satellite collected a vast amount of data that can be analyzed to provide derived techniques and information applicable to future missions.

MethaneAIR, is an aircraft-based precursor to MethaneSAT with similar spectroscopy and has by flown on ~75 flights from 2021 to 2024 in targeted regions of USA and Canada (Figure 1). Techniques developed to identify and quantify CH_4 emission sources using MethaneAIR data are transferable to MethaneSAT and other satellite platforms, with the MethaneAIR data being used to directly test MethaneSAT algorithms and for validation with coordinated campaigns. MethaneAIR flight data has been used successfully to quantify O&G point sources (Guanter et al., 2025; Chulakadabba et al., 2023). Using mosaic images Chulakadabba applied both a physics based, Integrated Mass enhancement (IME) and a Divergence Integral (DI) method to estimate emission rates. Both methods detect single blind controlled releases. The IME method, which used winds from weather simulations, was able to detect 200 kg h^{-1} while the DI was effective over 500 kg h^{-1} (Chulakadabba et al., 2023). Guanter et al. (2025) used an optimized processing chain to retrieve ΔXCH_4 (change in column-averaged methane concentration) on MethaneAIR L1B data (calibrated and georeferenced) showing the ability to detect plumes with emission rates of 120 kg h^{-1}. In this work we present a modification of the workflow used in Chulakadabba et al. (2023) by combining with the wavelet denoising method described by Zhang et al. (2024) via subsetting of area maps. This allows the far weaker CAFO plumes to not only be detected but quantified.

Whilst several aircraft-based campaigns have been performed to measure methane emissions over Oil and Gas (O&G) production (e.g. (Peischl et al., 2016; Karion et al., 2013; Chen et al., 2022), there are a limited number that have focused on Agricultural emissions. One study that separated aircraft derived Agricultural methane emissions from Oil and Gas was that by McCabe (2023) where they determined rates of 13 +- g of CH_4 $animal^{-1}$ h^{-1} for a single CAFO, which was considerably higher than reported in the EPA inventory. Background noise and wind speed are attributed as being major sources of uncertainty for plume detection (Saunois et al., 2024; Hancock

https://doi.org/10.5194/egusphere-2025-6237
Preprint. Discussion started: 12 February 2026
© Author(s) 2026. CC BY 4.0 License.

et al., 2025; Petrescu et al., 2024). Tedeschi et al (2022) emphasized the need to use both top-down and bottom-up methods to improve methane estimates.

2 Data and methods

This work quantifies agricultural plumes using a combination of MethaneAIR mosaics and known locations of CAFOs. Agricultural Scenes derived using these data are then processed using a wavelet denoising method to identify and mask plumes which are then quantified by the Divergence integral (DI) method. Robust plumes associated with CAFO's are quantified and discussed in relation to reported values from inventories and past studies.

2.1 Farm-list Development

The farm list comprises identified Concentrated Animal Feeding Operations (CAFOs), including their locations, types, and estimated maximum methane emissions. Site identification was initially guided by existing inventories (Maasakkers et al., 2023; Chang et al., 2021; European Commission, 2021), satellite imagery (Google Earth, © Google), and ClimateTrace data (Davitt et al., 2024). Verification was conducted using business information from Google Maps (© Google) and visible signage via Google Street View (© Google).

CAFOs were included if they were estimated to emit more than 100 kg CH_4 h^{-1}, equivalent to ~ 60000 - 20000 cattle depending on type and management, based on national emission factors and maximum reported livestock numbers(U.S. Environmental Protection Agency, 2024). Sites were also required to be sufficiently distant from oil and gas infrastructure to allow for source separation. Maximum livestock capacity was determined using the following hierarchy of data sources: (1) state-reported values, (2) self-reported data, (3) facility footprint and type, and (4) inventory estimates. Emissions were then calculated using EPA emission factors.

Each CAFO was assigned a unique numeric identifier. Prior to each MethaneAIR flight (2023), CAFOs near the planned flight path were were supplied to flight planners for them to be flown over if the mission would allow. After flight completion, additional CAFOs intersected by the actual flight paths were identified and added to the list, including smaller facilities.

https://doi.org/10.5194/egusphere-2025-6237
Preprint. Discussion started: 12 February 2026
© Author(s) 2026. CC BY 4.0 License.

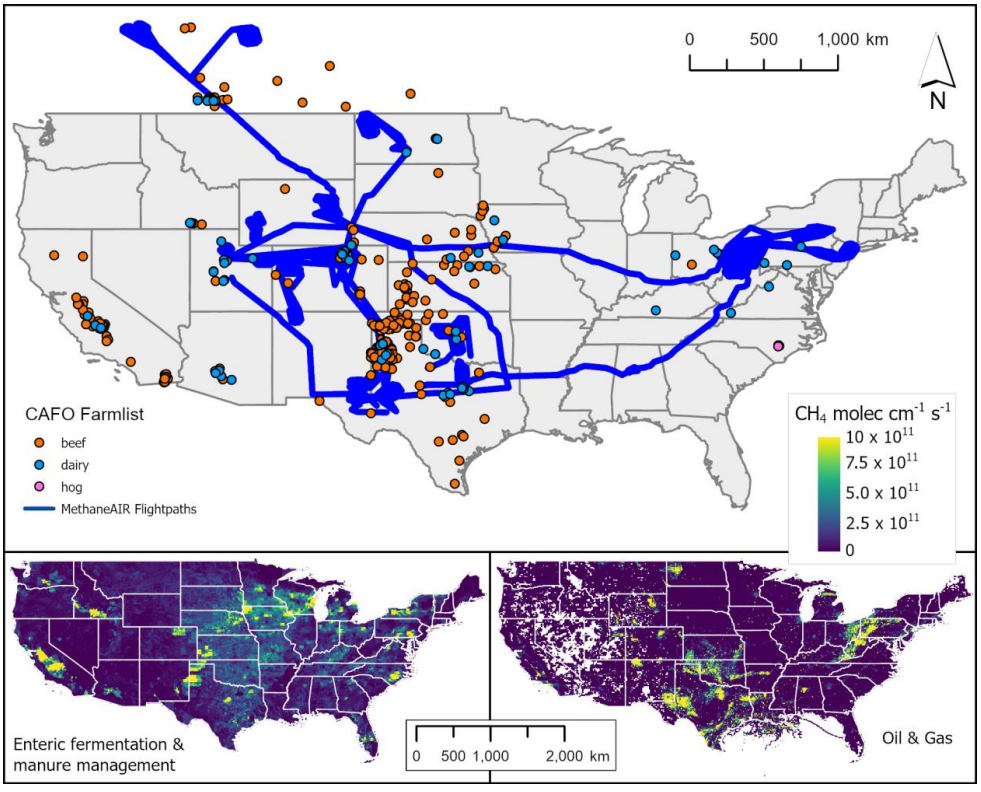

Figure 1: a) MethaneAIR flightpaths and Distribution of CAFO targets on initial Farm-list. (b) EPA gridded inventory field for combined enteric fermentation and manure management, and (c) oil & gas (Maasakkers et al., 2023). USA administrative boundaries from Esri.

2.2 MethaneAIR data

MethaneAIR uses a pair of grating spectrometers: one targeting absorption bands at 1.61 and 1.65 µm for CO_2 and CH_4 detection, and another at 1.27 µm for O_2, used to constrain the optical path length (Staebell et al., 2021). Installed and tested on NSF research aircraft in 2019 (Staebell et al., 2021), MethaneAIR operates at ~12 km altitude with a swath width of ~5.05 km and spatial resolution of ~ 6 × 20 m. Its design enables high retrieval precision (~17–20 ppb over flat terrain at 10m x 10m, (Chulakadabba et al., 2023) allowing the detection of both large and small methane emission sources which are often missed by coarser satellite instruments. This capability is essential for measuring methane emissions in complex environments such as oil and gas fields, landfills, and agricultural areas.

https://doi.org/10.5194/egusphere-2025-6237
Preprint. Discussion started: 12 February 2026
© Author(s) 2026. CC BY 4.0 License.

Level 3 (L3) data are delivered as gridded mosaics of column-averaged methane concentrations (XCH_4), derived using a CO_2 proxy retrieval algorithm that has been validated as a demonstration for the MethaneSAT mission (Chan Miller et al., 2024). A total of 75 flights conducted between 2021 and 2024 were available for analysis (Figure 1).

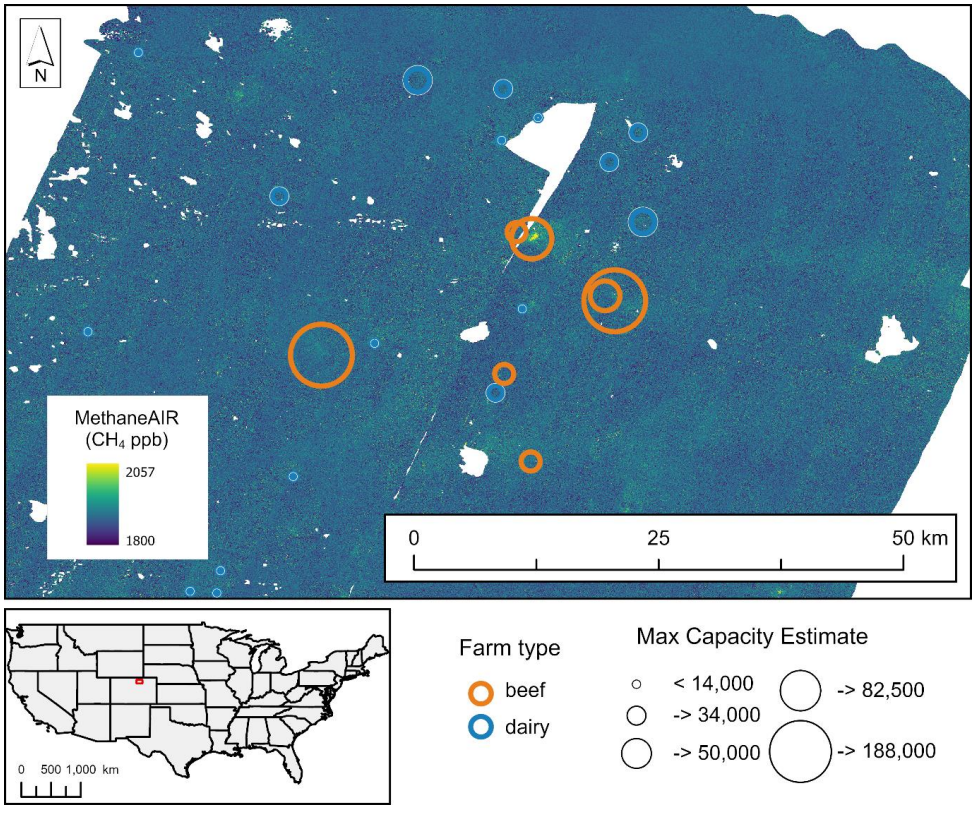

Figure 2: MethaneAIR flight mosaic from MethaneAIR flight MX050 over Denver, 2023-09-25 showing CAFOs in the area from the initial farm list. Maximum capacity values represent the registered animal capacity as reported by the Colorado Public Health and Environment (CDPHE, 2017). USA administrative boundaries from Esri.

2.3 Scene determination

To isolate agricultural emissions, MethaneAIR L3 mosaics (Figure 2) were subset around CAFO targets before applying wavelet denoising and the Divergence Integral (DI) method. This approach enhances the detectability of agricultural plumes, which might otherwise be statistically overshadowed by larger oil and gas emissions.

For each flight, CAFOs located within the mosaic extent were identified and then screened for quality. Cases were retained where no more than 2% of pixels within a ±0.005° (~500 m) buffer were masked, typically a result of cloud cover or close proximity to swath edge. For CAFOs meeting this threshold, an 'Agricultural Scene' was extracted as a ±0.02° subset of the Level 3 (L3) data centred on the CAFO. This process yielded 209 agricultural scenes associated with 84 unique CAFOs across 75 flights, examples of which are shown in Figure 1a, these scenes are then individually processed for plume detection and quantification.

https://doi.org/10.5194/egusphere-2025-6237
Preprint. Discussion started: 12 February 2026
© Author(s) 2026. CC BY 4.0 License.

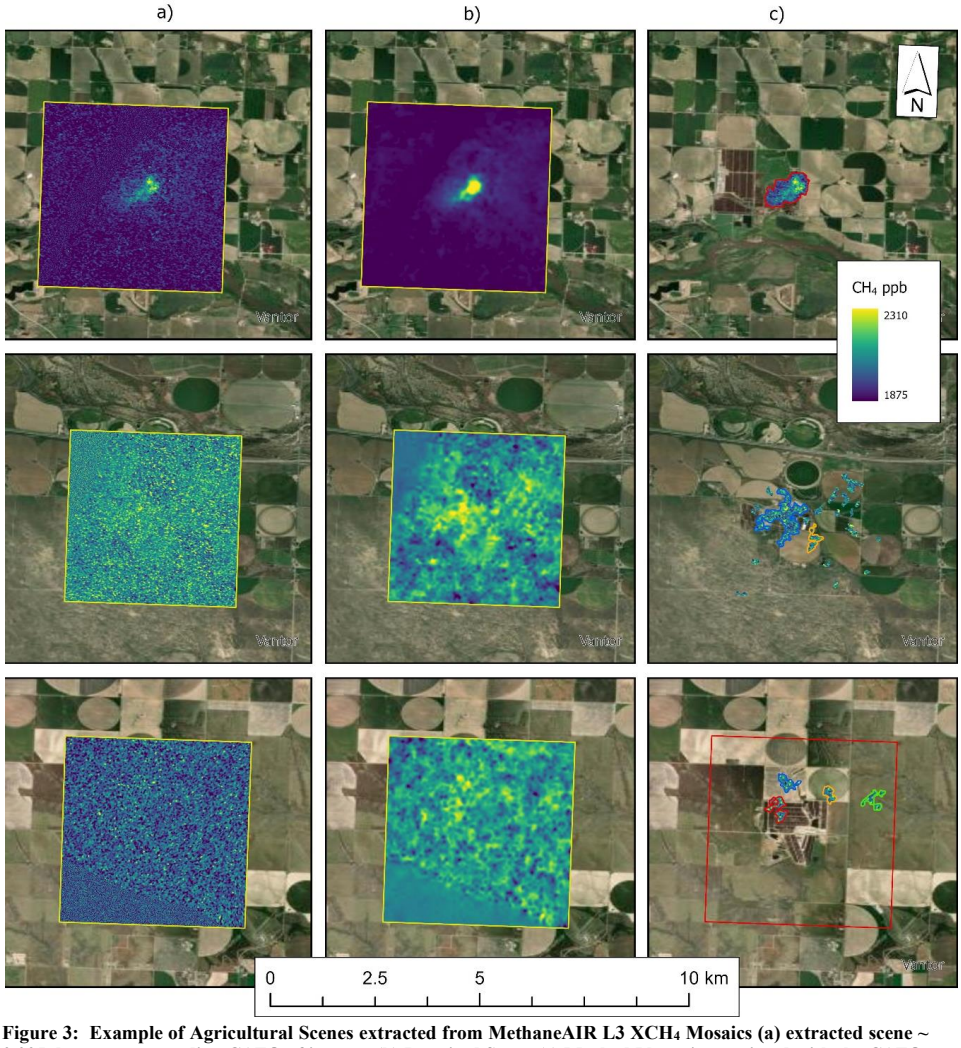

Figure 3: Example of Agricultural Scenes extracted from MethaneAIR L3 XCH_4 Mosaics (a) extracted scene ~ 0.005 degrees surrounding CAFO of interest (b) Denoised Scene (c) Masked Plume/s associated with the CAFO, with different colours denoting individual plumes. Imagery © Vantor, 2024.

2.4 Plume Detection and Quantification

175 The plume detection method uses a 2D discrete wavelet transform to denoise the methane concentration imagery (Figure 3). It separates image signals into low frequencies and high frequencies, so that the high-frequency noise can be subtracted to produce a clean image with enhanced plume signals. Binary plume masks are then generated using a combination of XCH_4 thresholding and a connected component algorithm. Additional filtering algorithms are applied to mitigate false detections. Subsequently, plume origins are determined based on plume morphology
180 and wind direction. Compared to the divergence integral plume detection method that was previously applied in MethaneAIR data (Warren et al., 2024), the wavelet-based method has higher performance in detecting low-

https://doi.org/10.5194/egusphere-2025-6237
Preprint. Discussion started: 12 February 2026
© Author(s) 2026. CC BY 4.0 License.

volume plumes (Zhang et al., 2026). Therefore, we use the wavelet-based detection method to maximize our plume finding capabilities in agricultural emissions. The combination of this approach with scene selection across a wide range of targets is somewhat novel outside of a controlled release setting. Unlike Cusworth et al. (2021) or Guanter et al. (2025) which apply detection algorithms across a the scene of the entire flight, limiting the scene sizes to just known locations allows for a finer distribution of concentrations for thresholding/percentile based identification methods. For flux quantification, the same divergence integral method in Chulakadabba et al. (2023) is applied as it has been validated by multiple controlled release tests. Firstly, a series of growing boxes is drawn around the plume origin. Then the surface flux divergence integral is computed for each box using wind fields from the High-Resolution Rapid Refresh model (NOAA, 2025) and the final flux is taken as the average of these values, with the uncertainty being the standard deviation. From the 209 agricultural scenes, 652 methane plumes were detected.

2.5 Plume Source Attribution

Each detected plume was manually evaluated to determine i) whether the source was agricultural (associated with a CAFO), ii) if it was unique, and iii) the likely on-farm source if apparent. For context, methane plume rasters were overlaid on high-resolution imagery from Google Earth (imagery © Google, 2024) to assess spatial alignment with the CAFO being considered. A plume was considered clearly associated with a CAFO when multiple qualitative indicators agreed, including proximity of the plume origin to the CAFO footprint, wind-consistent alignment, plume morphology, and the absence of nearby competing sources such as oil-and-gas infrastructure or adjacent CAFOs.

Uniqueness was assigned by visually checking for plume continuity; segments judged to be parts of a single contiguous plume were treated as one case (e.g. Figure 3c). While most plumes are clearly associated with the CAFO, it is not always possible to confidently determine the on-farm origin. Where possible, the specific on-farm source (e.g., lagoons or infrastructure) was identified, and a confidence level was assigned. Only plumes that can clearly be identified as coming from a Lagoon are flagged as such. Consequently, there will be many cases with Lagoon-related emissions remaining within the general agricultural category.

3 Results

A total of 209 agricultural scenes, encompassing 84 unique CAFO's including a mixture of beef, dairy and manure management operations, were analyzed using the wavelet denoising and DI method. This analysis resulted in 652 individual plume detections. However, the majority of these plumes were not attributable to the targeted CAFOs. Instead, they were typically associated with nearby oil and gas infrastructure, adjacent CAFOs, unidentified sources transported into the scene, or clearly a single plume that has been split (non-unique).

A total of 200 unique agricultural plumes were identified, of which 89 (44%) were classified as robust (Figure 4b). Robust plumes are defined as having a ratio of the standard deviation of the DI-derived flux to the flux itself of less than 1 (i.e., uncertainty below 100%). Although only 14% of detected plumes were both agricultural and

https://doi.org/10.5194/egusphere-2025-6237
Preprint. Discussion started: 12 February 2026
© Author(s) 2026. CC BY 4.0 License.

met the most stringent robustness criteria, nearly 40% of all scenes contained at least one robust plume. This demonstrates that the method is effective for detecting plumes at this scale, even within complex, mixed-source landscapes.

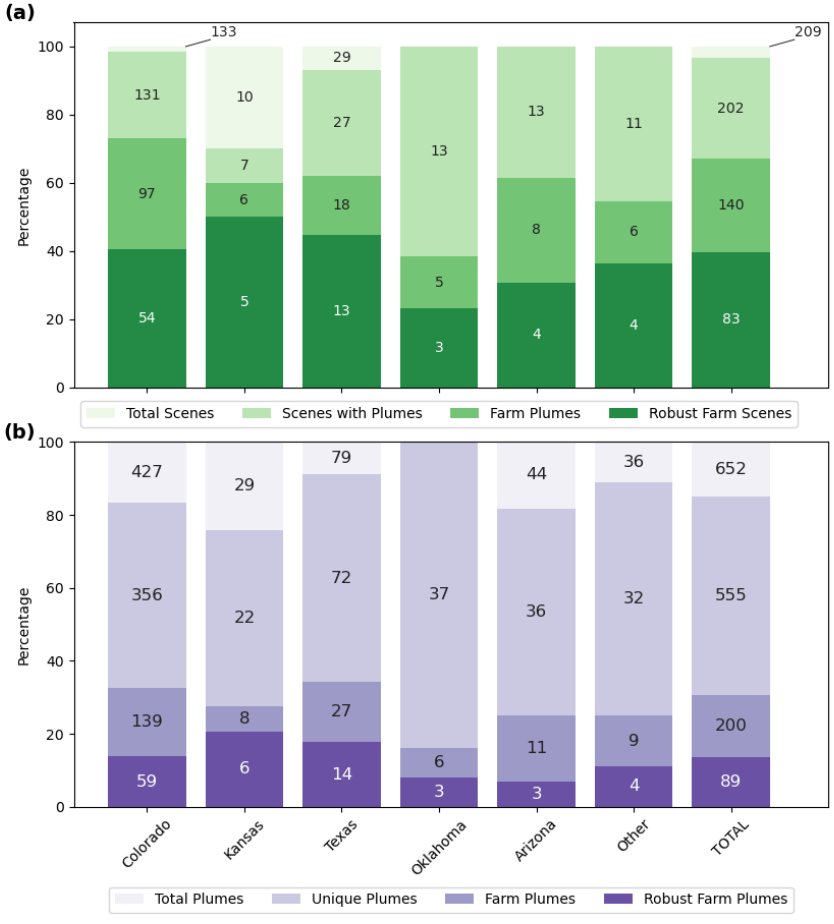

Figure 4. Summary of valid agricultural scenes (a) and associated plume detections (b), by state. Actual counts are displayed on each bar. Note: for Oklahoma, Arizona, and "Other," all valid scenes included plume detections. Additionally, all plumes detected in Oklahoma were classified as unique.

Given that Colorado had the highest number of robust agricultural scenes and plumes (Figure 4), it was a logical focal point for further analysis in this study. To better understand these results, accurate livestock population data is essential for estimating expected emissions from enteric fermentation and manure management. The most reliable and traceable dataset available for this analysis was the maximum capacity of registered and permitted

https://doi.org/10.5194/egusphere-2025-6237
Preprint. Discussion started: 12 February 2026
© Author(s) 2026. CC BY 4.0 License.

feedlots reported by the Colorado Department of Public Health and Environment (CDPHE, 2017). While the dataset is 7 years out of date for assessing emissions in 2024, it is still a consistent data source and in the absence of real-time animal counts, these maximum values were used as a proxy for estimating per-animal emissions. From the Colorado state inventory 2023 (CDPHE, 2023), the estimate state total methane emissions from enteric fermentation and manure management in 2017, were 0.227 and 0.0297 MMT of CH_4 respectively, rising modestly to 0.2286 (~7%) and 0.03497 (~17%) MMT CH_4 by 2020. Such trends may continue, and may be systematically reflected in the results from our analysis of MethaneAIR data

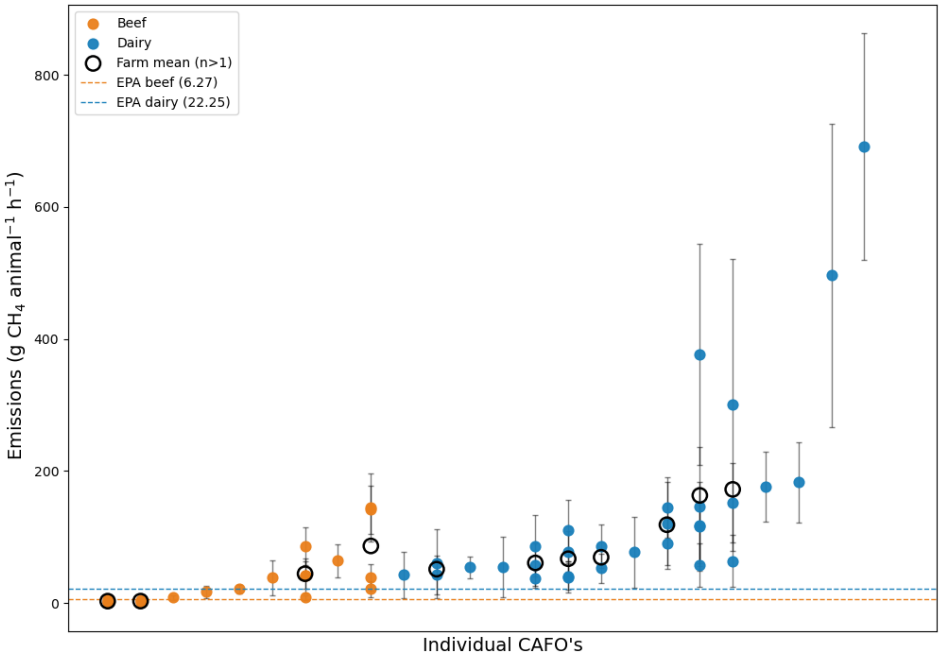

Figure 5. Methane emissions per animal for individual CAFO's, by type, and ranked low to high. Horizontal lines represent EPA per animal rates for Colorado state.

To compare emissions per animal values derived from MAIR to EPA we calculated the combined enteric fermentation and manure management emissions factors using the state specific data provided in Inventory of U.S. Greenhouse Gas Emissions and Sinks: 1990-2022 – Annexes (U.S. Environmental Protection Agency, 2024). For consistency across both source types, the reported state level values for the sources (tables A-151 and A-170) were divided by the state population (table A-124) using the values for dairy cows and beef on feedlot. This results in a total of 22.25 g CH_4 animal^{-1} h^{-1} for dairy and 6.57 g CH_4 animal^{-1} h^{-1} for beef. In the case of beef 90% of emissions are from enteric fermentation, whereas in dairy that value is 58%. Note that these values represent the mean of all operations, no matter the size, over the state of Colorado. Individually operations may have a wide range of emission factors.

These values were then compared to the total emissions for each scene. This was computed by averaging the robust, disconnected, non-unique plumes (i.e. the same plume) and summing the remaining unique plumes within

https://doi.org/10.5194/egusphere-2025-6237
Preprint. Discussion started: 12 February 2026
© Author(s) 2026. CC BY 4.0 License.

the scene to give total operational emissions. Overall Beef CAFOs, on average, exhibited lower emissions per animal than dairy operations, although substantial variability was observed across both types (Figure 5). A Welch's t-test indicated beef values were significantly lower than dairy values, $t(33.86) = -4.02$, $p = 0.00031$. Because CAFOs may not always operate at their permitted maximum capacity, methane emissions derived from MethaneAIR observations could fall below EPA per-animal emission factors simply due to fewer animals being present than the stated capacity. This pattern was largely met for beef operations, where most emission estimates ranged between 0 and 10 g CH_4 animal^{-1} h^{-1} — in line with EPA's estimate of 6.57 g CH_4 animal^{-1} h^{-1} (Figure 5).

In contrast, dairy operations exhibited higher emissions, with most estimates falling between 40 and 80 g CH_4 animal^{-1} h^{-1}. This discrepancy may suggest that beef CAFOs typically operate below their permitted capacity, whereas dairy CAFOs may be functioning closer to permitted capacity. Alternatively, the elevated emissions observed in dairy operations may reflect a greater contribution from manure management systems, which are known to exhibit high variability. It is also important to consider that the EPA emission factors represent annual averages, whereas MethaneAIR captures instantaneous emissions. Although some diurnal and seasonal variability is expected, the consistency and magnitude of the dairy results suggest an additional contributing factor.

	Reported (Enteric fermentation + Manure management)		**Measured** (Total farm-level emissions)		
CAFO Type	EPA Colorado	IPCC (Tier 2, USA)	Goltson et al. (landbased)	McCabe et al.* (aircraft)	MethaneAIR (mean)
Beef	6.67	~6.62	9.48 ± 0.93	13 ± 2	34.80 ± 4.49
Dairy	22.25	~13.95	39.32 ± 2.92		122.32 ± 13.62

Table 1 Approximate CH_4 emissions (g animal^{-1} h^{-1}), reported from EPA, IPCC defaults, and values obtained for Colorado state covered by MethaneAIR flights for this study. *McCabe et al. (2023) focussed primarily on beef feedlots but included a small number of dairy operations.

Averaging over all Colorado scenes (Table 1), our results indicate average emissions of 34.80 g animal^{-1} h^{-1} for beef cattle and 122.32 g animal^{-1} h^{-1} for dairy cattle, which exceeds the EPA's Tier 2 inventory estimates of 6.67 g animal^{-1} h^{-1} for beef and 22.25 g animal^{-1} h^{-1} for dairy. The median values are, however, lower at 19.23 g animal^{-1} h^{-1} and 86.61 g animal^{-1} h^{-1} but remain above EPA values. Other studies conducted in northeastern Colorado also report lower values: Golston et al. (2020) measured 9.48 ± 0.93 g animal^{-1} h^{-1} for beef and 39.32 ± 2.92 g animal^{-1} h^{-1} for dairy using mobile labs during summer, while McCabe et al. (2023) reported a blended average of 13± 2 g animal^{-1} h^{-1} across the two CAFOs type. Additionally, Yu et al. (2021) used aircraft-based inversions to quantify methane emissions across the Upper Midwest and found that livestock emissions were approximately 25% higher than EPA estimates during summer and winter, though their approach focused on regional fluxes rather than plume-based facility attribution

https://doi.org/10.5194/egusphere-2025-6237
Preprint. Discussion started: 12 February 2026
© Author(s) 2026. CC BY 4.0 License.

To validate EPA and other studies methane emission estimates from CAFOs, a deeper understanding of actual CAFO activity—beyond consented capacity—is essential. The current results are plausible and align with expectations, showing clear differences between beef and dairy operations. However, several outliers in both categories exhibit emissions far exceeding EPA estimates. While these cannot be directly attributed without more detailed farm-level data, further work could be conducted to investigate the conditions under which these anomalies occur to identify potential biases.

3.1 Detection Thresholds

To assess reliability and frequency of observation, detection thresholds were evaluated using plume detection rates under varying conditions, focusing on estimated emission size and meteorological factors such as wind speed.

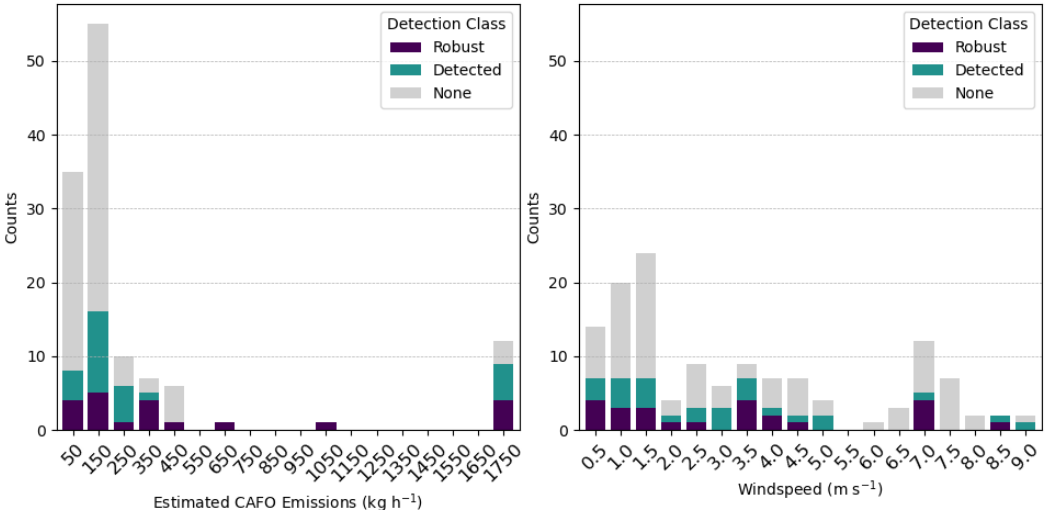

Figure 6. MethaneAIR scene-based plume detection rates for estimated emission size (left) and windspeed (right) for concentrated animal feeding operations (CAFOs) in Northeast Colorado

Figure 6 shows the rate of plume and robust plume detection as a function of estimated CAFO emissions (based upon permitted animal numbers and detected emission rates) and windspeed for the Colorado subset. Unsurprisingly, the overwhelming number of negative detections (None) occur at low expected emission rates based on CDPHE data (CDPHE, 2017), there are however a significant number of positive and robust detections in this range too. The meteorological features are more nuanced, with wind speed showing modest increase in negative detections at low and high wind speeds. Again, this makes sense intuitively, at high windspeeds, there will be less buildup of methane, making plumes harder to detect, at low wind speeds the increased build up may no longer be plume like. Temperature and preceding rainfall were also investigated but did not show significant relationships due to the limited number of observations.

https://doi.org/10.5194/egusphere-2025-6237
Preprint. Discussion started: 12 February 2026
© Author(s) 2026. CC BY 4.0 License.

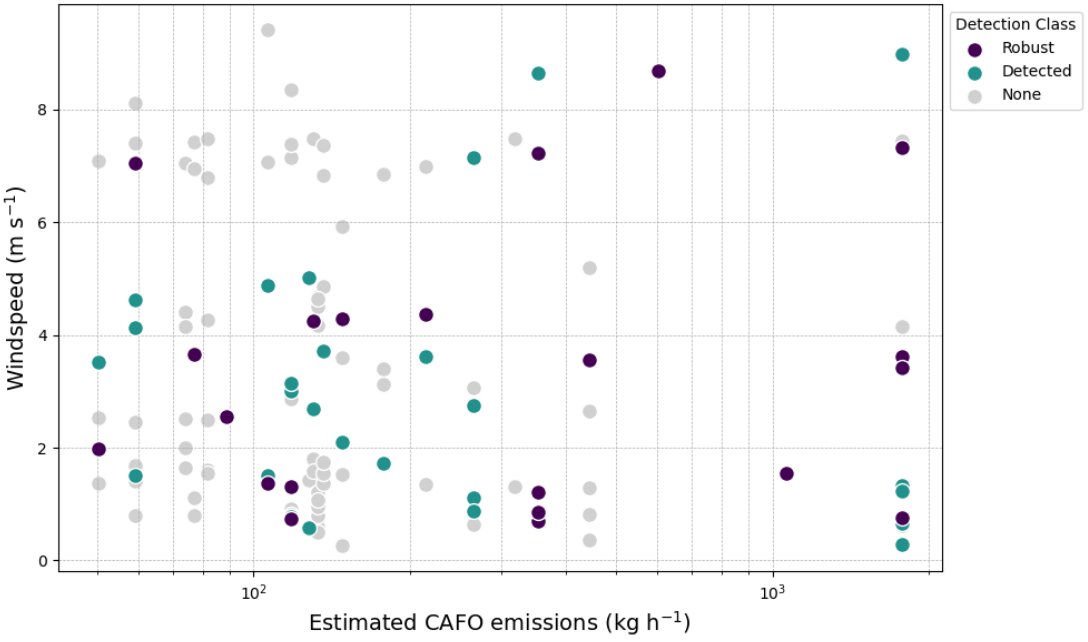

Figure 7. Detection class as a function of estimated emissions and windspeed

The relationship between emission rate, wind speed, and detection performance was evaluated across three detection classes (Figure 7). While the limited sample size precludes the development of statistically robust, dynamic detection thresholds several trends are evident.

Detection and reliable quantification of emission sources emitting less than 100 kg h^{-1} are occasionally achievable when wind speeds range between 2 and 6 m s^{-1}. Within this wind speed window, the atmospheric transport conditions appear favourable for plume detection. At higher emission rates, particularly above 200 kg h^{-1}, the influence of wind speed on detection success diminishes, suggesting that stronger sources are more readily detectable regardless of moderate variations in wind conditions.

A subset of failed or non-robust detections occurred despite satisfying the nominal wind speed and emission rate criteria. These anomalies may be attributed to several factors, including temporal variability in actual emission rates, discrepancies between modelled wind data (e.g., HRRR) and on-site wind conditions, and elevated background methane concentrations that may obscure the signal from emission sources.

3.2 Emission Variability Drivers

We can extend this analysis to explore the variability in observed, robust methane emissions from CAFOs, as in the detection case we focus only on the influence of windspeed. Although the dataset is limited, most outliers occurred during high windspeed conditions. While this pattern may reflect a windspeed-related bias in the emission estimation methodology, it is notable that several high-wind cases exhibited minimal emission enhancements, suggesting site-specific behavior (Figure 8).

https://doi.org/10.5194/egusphere-2025-6237
Preprint. Discussion started: 12 February 2026
© Author(s) 2026. CC BY 4.0 License.

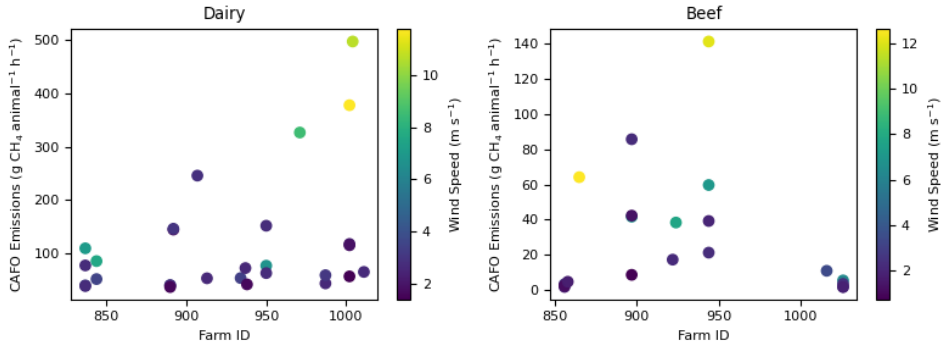

Figure 8. Methane emissions per animal (g h^{-1}) from dairy (left) and beef (right) concentrated animal feeding operations (CAFOs) in Northeast Colorado.

For two CAFOs (Farm 1000 and Farm 950) with repeated observations across a range of wind conditions, elevated emissions were only detected during periods of high wind speed. At other sites, however, high winds did not correspond to increased enhancements. Together, these observations indicate that high windspeed alone does not consistently produce larger observed enhancements. This pattern suggests that facility-specific factors likely influence emission responsiveness to wind, and that the windspeed-emission relationship may be site-specific, and shaped by the intermittent, weather-dependent nature of emissions from lagoon-based systems.

The site-dependent nature of the wind–emission relationship aligns with previous studies showing that methane emissions from lagoon-based systems can respond strongly to weather events. Leytem et al. (2017) demonstrated that wind events, alongside rainfall and freeze/thaw cycles, significantly increased CH_4 emissions from dairy lagoons in Idaho, independent of temperature. Their models identified windspeed as a key predictor. Confirming this wind-driven variability more robustly would require expanded aerial surveys, improved traceability of CAFO-related EPA data beyond Colorado, or additional facility operation data.

Other studies have identified several factors influencing variability of CH_4 emissions from farms, including barn temperature and humidity (Ouatahar et al., 2024), manure management practice, diurnal variability due to temp and other atmospheric conditions (Golston et al., 2020; Ouatahar et al., 2024). Golston et al. also reported substantial spatial variability within facilities. Dietary influence can also be significant. Yu et al. (2021) suggested that management practices had a stronger influence than seasonality accounted for in bottom-up approaches; for example, anaerobic lagoons produce significant emissions, and the length of time the manure is stored in them following removal from housing can have an impact.

4 Conclusions and Implications

This study demonstrates the effectiveness of MethaneAIR in detecting and quantifying methane emissions from CAFOs in Northeast Colorado. A total of 652 methane plumes were identified across 209 agricultural scenes, with 89 (42%) of scenes yielding at least one robust CAFO related plume. These results highlight the potential as well

https://doi.org/10.5194/egusphere-2025-6237
Preprint. Discussion started: 12 February 2026
© Author(s) 2026. CC BY 4.0 License.

as the complexity of isolating agricultural emissions in regions with overlapping oil and gas infrastructure and underscore the importance of targeted analytical approaches.

A central methodology of this work is agricultural scene extraction prior to further processing, which isolates CAFO-associated emissions from broader MethaneAIR flight mosaics. By spatially subsetting the data around known CAFO locations and filtering out scenes with insufficient data coverage, this approach enhances the detectability of smaller, diffuse agricultural plumes that would otherwise be statistically overshadowed by dominant oil and gas emissions. This method improves attribution accuracy and provides a scalable framework for future airborne and satellite-based methane monitoring in mixed-source landscapes.

As anticipated, our analysis revealed that dairy CAFOs generally emit more methane per animal than beef operations, with many exceeding EPA emission factor estimates—likely due to higher operational intensity or greater contributions from manure management systems. In contrast, beef CAFOs typically emitted below EPA estimates, suggesting under-capacity operation or less intensive waste management practices. These findings align with previous aircraft-based studies (Yu et al., 2021; McCabe et al., 2023) and highlight the limitations of static emission factors in capturing real-world variability. Additional flights and more importantly, detailed on-farm data, such as true stocking rates and waste practices, are be needed to tie the observed emissions to the underlying activity, thus allowing the verification of emission factors.

Windspeed emerged as the dominant meteorological factor influencing plume detectability. Emissions below 100 kg CH_4 h^{-1} were possible, but not consistently, detected when windspeed ranged between 2 and 6 m s^{-1}, while higher emissions were detectable across a broader range. However, the relationship between windspeed and emissions varied by site, suggesting that emission dynamics are influenced by localized infrastructure, management practices, and lagoon behaviour.

This study focused on one region and relied on coincident CAFO location data. Broader application will require validation across additional regions and incorporation of farm-specific information.

These findings provide critical insights for top-down methane monitoring efforts. Although MethaneSAT is no longer operational, the agricultural scene extraction and attribution strategies developed here remain highly relevant for other current and future missions. This approach offers an operational blueprint for applying airborne and spaceborne sensors in agricultural regions. By advancing understanding of methane emissions from CAFOs, this work establishes a methodological foundation for integrating airborne and satellite observations into agricultural methane monitoring, inventory improvement, and mitigation studies.

Code/Data availability

Python code used for data analyses and visualizations can be obtained from the corresponding authors upon reasonable request. MethaneAIR point source data can be accessed online from the Earth Engine Data Catalog at https://developers.google.com/earth-engine/datasets/tags/methaneair (Earth Engine Data Catalog, 2025).

Author contribution

PS led the writing of the manuscript, incorporating comments and revisions from all authors, and produced several key figures and analyses. AG developed the processing methods presented in this work and contributed to the manuscript and figure generation. ZZ developed the wavelet denoising approach, building on the DI flux estimates

https://doi.org/10.5194/egusphere-2025-6237
Preprint. Discussion started: 12 February 2026
© Author(s) 2026. CC BY 4.0 License.

produced by AC and MS. MS, JEF, and SCW oversaw campaign planning, instrument calibration, and data processing. SMF, JW, JR, and all other authors provided valuable insights and interpretations throughout the research and the preparation of the manuscript.

Competing interests

The contact author has declared that none of the authors has any competing interests.

References

CDPHE: Feedlot registration and compliance data, Colorado Department of Public Health Environment - Environmental Agriculture Program., 2017.

CDPHE: Colorado Greenhouse Gas Inventory Report, Colorado Department of Public Health and Environment, 2023.

Chan Miller, C., Roche, S., Wilzewski, J. S., Liu, X., Chance, K., Souri, A. H., Conway, E., Luo, B., Samra, J., Hawthorne, J., Sun, K., Staebell, C., Chulakadabba, A., Sargent, M., Benmergui, J. S., Franklin, J. E., Daube, B. C., Li, Y., Laughner, J. L., Baier, B. C., Gautam, R., Omara, M., and Wofsy, S. C.: Methane retrieval from MethaneAIR using the CO2 proxy approach: a demonstration for the upcoming MethaneSAT mission, Atmos. Meas. Tech., 17, 5429–5454, 10.5194/amt-17-5429-2024, 2024.

Chang, J., Peng, S., Yin, Y., Ciais, P., Havlik, P., and Herrero, M.: The Key Role of Production Efficiency Changes in Livestock Methane Emission Mitigation, AGU Advances, 2, e2021AV000391, https://doi.org/10.1029/2021AV000391, 2021.

Chen, Y., Sherwin, E. D., Berman, E. S. F., Jones, B. B., Gordon, M. P., Wetherley, E. B., Kort, E. A., and Brandt, A. R.: Quantifying Regional Methane Emissions in the New Mexico Permian Basin with a Comprehensive Aerial Survey, Environmental Science & Technology, 56, 4317–4323, 10.1021/acs.est.1c06458, 2022.

Chulakadabba, A., Sargent, M., Lauvaux, T., Benmergui, J. S., Franklin, J. E., Chan Miller, C., Wilzewski, J. S., Roche, S., Conway, E., Souri, A. H., Sun, K., Luo, B., Hawthrone, J., Samra, J., Daube, B. C., Liu, X., Chance, K., Li, Y., Gautam, R., Omara, M., Rutherford, J. S., Sherwin, E. D., Brandt, A., and Wofsy, S. C.: Methane point source quantification using MethaneAIR: a new airborne imaging spectrometer, Atmos. Meas. Tech., 16, 5771–5785, 10.5194/amt-16-5771-2023, 2023.

Cusworth, D. H., Bloom, A. A., Ma, S., Miller, C. E., Bowman, K., Yin, Y., Maasakkers, J. D., Zhang, Y., Scarpelli, T. R., Qu, Z., Jacob, D. J., and Worden, J. R.: A Bayesian framework for deriving sector-based methane emissions from top-down fluxes, Communications Earth & Environment, 2, 242, 10.1038/s43247-021-00312-6, 2021.

Davitt, A., Lewis, C., Andoe-Leggett, M., and Schiller, S.: Agriculture sector- Countrylevel Enteric fermentation and Manure Management Emissions Estimates from Cattle Operations. WattTime, USA and Carbon Yield, USA. [dataset], 2024.

European Commission, J. R. C. N. E. A. A.: EDGAR v6.0 Global Emissions, European Commission, Joint Research Centre (JRC), 2021.

Golston, L. M., Pan, D., Sun, K., Tao, L., Zondlo, M. A., Eilerman, S. J., Peischl, J., Neuman, J. A., and Floerchinger, C.: Variability of Ammonia and Methane Emissions from Animal Feeding Operations in Northeastern Colorado, Environmental Science & Technology, 54, 11015–11024, 10.1021/acs.est.0c00301, 2020.

Guanter, L., Warren, J., Omara, M., Chulakadabba, A., Roger, J., Sargent, M., Franklin, J. E., Wofsy, S. C., and Gautam, R.: Remote sensing of methane point sources with the MethaneAIR airborne spectrometer, EGUsphere, 2025, 1–22, 10.5194/egusphere-2024-3577, 2025.

Hancock, S. E., Jacob, D. J., Chen, Z., Nesser, H., Davitt, A., Varon, D. J., Sulprizio, M. P., Balasus, N., Estrada, L. A., Cazorla, M., Dawidowski, L., Diez, S., East, J. D., Penn, E., Randles, C. A., Worden, J., Aben, I., Parker, R. J., and Maasakkers, J. D.: Satellite quantification of methane emissions from South American countries: a high-resolution inversion of TROPOMI and GOSAT observations, Atmos. Chem. Phys., 25, 797–817, 10.5194/acp-25-797-2025, 2025.

IPCC: 2006 IPCC Guidelines for National Greenhouse Gas Inventories, IPCC, 2006.

IPCC: 2019 Refinement to the 2006 IPCC Guidelines for National Greenhouse Gas Inventories, IPCC, 2019.

IPCC: Sections. In: Climate Change 2023: Synthesis Report. Contribution of Working Groups I, II and III to the Sixth
Assessment Report of the Intergovernmental Panel on Climate Change IPCC, Geneva, Switzerland, 35–115, doi: 10.59327/IPCC/AR6-9789291691647, 2023.

https://doi.org/10.5194/egusphere-2025-6237
Preprint. Discussion started: 12 February 2026
© Author(s) 2026. CC BY 4.0 License.

Jacob, D. J., Turner, A. J., Maasakkers, J. D., Sheng, J., Sun, K., Liu, X., Chance, K., Aben, I., McKeever, J., and Frankenberg, C.: Satellite observations of atmospheric methane and their value for quantifying methane emissions, Atmos. Chem. Phys., 16, 14371–14396, 10.5194/acp-16-14371-2016, 2016.

Jacob, D. J., Varon, D. J., Cusworth, D. H., Dennison, P. E., Frankenberg, C., Gautam, R., Guanter, L., Kelley, J., McKeever, J., Ott, L. E., Poulter, B., Qu, Z., Thorpe, A. K., Worden, J. R., and Duren, R. M.: Quantifying methane emissions from the global scale down to point sources using satellite observations of atmospheric methane, Atmos. Chem. Phys., 22, 9617–9646, 10.5194/acp-22-9617-2022, 2022.

Karion, A., Sweeney, C., Pétron, G., Frost, G., Michael Hardesty, R., Kofler, J., Miller, B. R., Newberger, T., Wolter, S., Banta, R., Brewer, A., Dlugokencky, E., Lang, P., Montzka, S. A., Schnell, R., Tans, P., Trainer, M., Zamora, R., and Conley, S.: Methane emissions estimate from airborne measurements over a western United States natural gas field, Geophysical Research Letters, 40, 4393–4397, https://doi.org/10.1002/grl.50811, 2013.

Leytem, A. B., Bjorneberg, D. L., Koehn, A. C., Moraes, L. E., Kebreab, E., and Dungan, R. S.: Methane emissions from dairy lagoons in the western United States, Journal of Dairy Science, 100, 6785–6803, https://doi.org/10.3168/jds.2017-12777, 2017.

Li, F., Bai, S., Lin, K., Feng, C., Sun, S., Zhao, S., Wang, Z., Zhou, W., Zhou, C., and Zhang, Y.: Satellite-Based Surveys Reveal Substantial Methane Point-Source Emissions in Major Oil & Gas Basins of North America During 2022–2023, Journal of Geophysical Research: Atmospheres, 129, e2024JD040870, https://doi.org/10.1029/2024JD040870, 2024.

Maasakkers, J. D., Jacob, D. J., Sulprizio, M. P., Scarpelli, T. R., Nesser, H., Sheng, J. X., Zhang, Y., Hersher, M., Bloom, A. A., Bowman, K. W., Worden, J. R., Janssens-Maenhout, G., and Parker, R. J.: Global distribution of methane emissions, emission trends, and OH concentrations and trends inferred from an inversion of GOSAT satellite data for 2010–2015, Atmos. Chem. Phys., 19, 7859–7881, 10.5194/acp-19-7859-2019, 2019.

Maasakkers, J. D., McDuffie, E. E., Sulprizio, M. P., Chen, C., Schultz, M., Brunelle, L., Thrush, R., Steller, J., Sherry, C., Jacob, D. J., Jeong, S., Irving, B., and Weitz, M.: A Gridded Inventory of Annual 2012–2018 U.S. Anthropogenic Methane Emissions, Environmental Science & Technology, 57, 16276–16288, 10.1021/acs.est.3c05138, 2023.

McCabe, M. E., Pollack, I. B., Fischer, E. V., Steinmann, K. M., and Caulton, D. R.: Technical note: Isolating methane emissions from animal feeding operations in an interfering location, Atmos. Chem. Phys., 23, 7479–7494, 10.5194/acp-23-7479-2023, 2023.

Mead, G. J., Herman, D. I., Giorgetta, F. R., Malarich, N. A., Baumann, E., Washburn, B. R., Newbury, N. R., Coddington, I., and Cossel, K. C.: Apportionment and Inventory Optimization of Agriculture and Energy Sector Methane Emissions Using Multi-Month Trace Gas Measurements in Northern Colorado, Geophysical Research Letters, 51, e2023GL105973, https://doi.org/10.1029/2023GL105973, 2024.

Michel, S. E., Lan, X., Miller, J., Tans, P., Clark, J. R., Schaefer, H., Sperlich, P., Brailsford, G., Morimoto, S., Moossen, H., and Li, J.: Rapid shift in methane carbon isotopes suggests microbial emissions drove record high atmospheric methane growth in 2020–2022, Proceedings of the National Academy of Sciences, 121, e2411212121, doi:10.1073/pnas.2411212121, 2024.

National Academies of Sciences: Improving characterization of anthropogenic methane emissions in the United States, National Academies Press2018.

NOAA: High-Resolution Rapid Refresh (HRRR) Model, Registry of Open Data on AWS [dataset], 2025.

Ouatahar, L., Bannink, A., Zentek, J., Amon, T., Deng, J., Hempel, S., Janke, D., Beukes, P., van der Weerden, T., Krol, D., Lanigan, G. J., and Amon, B.: An integral assessment of the impact of diet and manure management on whole-farm greenhouse gas and nitrogen emissions in dairy cattle production systems using process-based models, Waste Management, 187, 79–90, https://doi.org/10.1016/j.wasman.2024.07.007, 2024.

Peischl, J., Karion, A., Sweeney, C., Kort, E. A., Smith, M. L., Brandt, A. R., Yeskoo, T., Aikin, K. C., Conley, S. A., Gvakharia, A., Trainer, M., Wolter, S., and Ryerson, T. B.: Quantifying atmospheric methane emissions from oil and natural gas production in the Bakken shale region of North Dakota, Journal of Geophysical Research: Atmospheres, 121, 6101–6111, https://doi.org/10.1002/2015JD024631, 2016.

Petrescu, A. M. R., Peters, G. P., Engelen, R., Houweling, S., Brunner, D., Tsuruta, A., Matthews, B., Patra, P. K., Belikov, D., Thompson, R. L., Höglund-Isaksson, L., Zhang, W., Segers, A. J., Etiope, G., Ciotoli, G., Peylin, P., Chevallier, F., Aalto, T., Andrew, R. M., Bastviken, D., Berchet, A., Broquet, G., Conchedda, G., Dellaert, S. N. C., Denier van der Gon, H., Gütschow, J., Haussaire, J. M., Lauerwald, R., Markkanen, T., van Peet, J. C. A., Pison, I., Regnier, P., Solum, E., Scholze, M., Tenkanen, M., Tubiello, F. N., van der Werf, G. R., and Worden, J. R.: Comparison of observation- and inventory-based methane emissions for eight large global emitters, Earth Syst. Sci. Data, 16, 4325–4350, 10.5194/essd-16-4325-2024, 2024.

Roques, S., Martinez-Fernandez, G., Ramayo-Caldas, Y., Popova, M., Denman, S., Meale, S. J., and Morgavi, D. P.: Recent Advances in Enteric Methane Mitigation and the Long Road to Sustainable Ruminant Production, Annual Review of Animal Biosciences, 12, 321–343, https://doi.org/10.1146/annurev-animal-021022-024931, 2024.

Saunois, M., Martinez, A., Poulter, B., Zhang, Z., Raymond, P., Regnier, P., Canadell, J. G., Jackson, R. B., Patra, P. K., Bousquet, P., Ciais, P., Dlugokencky, E. J., Lan, X., Allen, G. H., Bastviken, D., Beerling, D. J., Belikov,

https://doi.org/10.5194/egusphere-2025-6237
Preprint. Discussion started: 12 February 2026
© Author(s) 2026. CC BY 4.0 License.

D. A., Blake, D. R., Castaldi, S., Crippa, M., Deemer, B. R., Dennison, F., Etiope, G., Gedney, N., Höglund-Isaksson, L., Holgerson, M. A., Hopcroft, P. O., Hugelius, G., Ito, A., Jain, A. K., Janardanan, R., Johnson, M. S., Kleinen, T., Krummel, P., Lauerwald, R., Li, T., Liu, X., McDonald, K. C., Melton, J. R., Mühle, J., Müller, J., Murguia-Flores, F., Niwa, Y., Noce, S., Pan, S., Parker, R. J., Peng, C., Ramonet, M., Riley, W. J., Rocher-Ros, G., Rosentreter, J. A., Sasakawa, M., Segers, A., Smith, S. J., Stanley, E. H., Thanwerdas, J., Tian, H., Tsuruta, A., Tubiello, F. N., Weber, T. S., van der Werf, G., Worthy, D. E., Xi, Y., Yoshida, Y., Zhang, W., Zheng, B., Zhu, Q., Zhu, Q., and Zhuang, Q.: Global Methane Budget 2000-2020, Earth Syst. Sci. Data Discuss., 2024, 1–147, 10.5194/essd-2024-115, 2024.

Schuit, B. J., Maasakkers, J. D., Bijl, P., Mahapatra, G., van den Berg, A. W., Pandey, S., Lorente, A., Borsdorff, T., Houweling, S., Varon, D. J., McKeever, J., Jervis, D., Girard, M., Irakulis-Loitxate, I., Gorroño, J., Guanter, L., Cusworth, D. H., and Aben, I.: Automated detection and monitoring of methane super-emitters using satellite data, Atmos. Chem. Phys., 23, 9071–9098, 10.5194/acp-23-9071-2023, 2023.

Sherwin, E. D., El Abbadi, S. H., Burdeau, P. M., Zhang, Z., Chen, Z., Rutherford, J. S., Chen, Y., and Brandt, A. R.: Single-blind test of nine methane-sensing satellite systems from three continents, Atmos. Meas. Tech., 17, 765–782, 10.5194/amt-17-765-2024, 2024.

Staebell, C., Sun, K., Samra, J., Franklin, J., Chan Miller, C., Liu, X., Conway, E., Chance, K., Milligan, S., and Wofsy, S.: Spectral calibration of the MethaneAIR instrument, Atmos. Meas. Tech., 14, 3737–3753, 10.5194/amt-14-3737-2021, 2021.

Tedeschi, L. O., Abdalla, A. L., Álvarez, C., Anuga, S. W., Arango, J., Beauchemin, K. A., Becquet, P., Berndt, A., Burns, R., De Camillis, C., Chará, J., Echazarreta, J. M., Hassouna, M., Kenny, D., Mathot, M., Mauricio, R. M., McClelland, S. C., Niu, M., Onyango, A. A., Parajuli, R., Pereira, L. G. R., Del Prado, A., Paz Tieri, M., Uwizeye, A., and Kebreab, E.: Quantification of methane emitted by ruminants: a review of methods, J Anim Sci, 100, 10.1093/jas/skac197, 2022.

U.S. Environmental Protection Agency: Inventory of U.S. Greenhouse Gas Emissions and Sinks: 1990–2022 – Annexes, 2024.

Varon, D. J., Jacob, D. J., McKeever, J., Jervis, D., Durak, B. O. A., Xia, Y., and Huang, Y.: Quantifying methane point sources from fine-scale satellite observations of atmospheric methane plumes, Atmos. Meas. Tech., 11, 5673–5686, 10.5194/amt-11-5673-2018, 2018.

Warren, J. D., Sargent, M., Williams, J. P., Omara, M., Miller, C. C., Roche, S., MacKay, K., Manninen, E., Chulakadabba, A., Himmelberger, A., Benmergui, J., Zhang, Z., Guanter, L., Wofsy, S., and Gautam, R.: Sectoral contributions of high-emitting methane point sources from major U.S. onshore oil and gas producing basins using airborne measurements from MethaneAIR, EGUsphere, 2024, 1–22, 10.5194/egusphere-2024-3865, 2024.

Wójcik-Gront, E. and Wnuk, A.: Evaluating Methane Emission Estimates from Intergovernmental Panel on Climate Change Compared to Sentinel-Derived Air–Methane Data, 10.3390/su17030850, 2025.

Worden, J. R., Cusworth, D. H., Qu, Z., Yin, Y., Zhang, Y., Bloom, A. A., Ma, S., Byrne, B. K., Scarpelli, T., Maasakkers, J. D., Crisp, D., Duren, R., and Jacob, D. J.: The 2019 methane budget and uncertainties at 1° resolution and each country through Bayesian integration Of GOSAT total column methane data and a priori inventory estimates, Atmos. Chem. Phys., 22, 6811–6841, 10.5194/acp-22-6811-2022, 2022.

Yu, X., Millet, D. B., Wells, K. C., Henze, D. K., Cao, H., Griffis, T. J., Kort, E. A., Plant, G., Deventer, M. J., Kolka, R. K., Roman, D. T., Davis, K. J., Desai, A. R., Baier, B. C., McKain, K., Czarnetzki, A. C., and Bloom, A. A.: Aircraft-based inversions quantify the importance of wetlands and livestock for Upper Midwest methane emissions, Atmos. Chem. Phys., 21, 951–971, 10.5194/acp-21-951-2021, 2021.

Zhang, Z., Sargent, M., Benmergui, J., and Wofsy, S. C.: Automatic Methane Point Source Plume Masking Based on Wavelet Transform Image Processing, AGU24, Washington, D.C., 2024/12/10,

Zhang, Z., Sargent, M., Warren, J. D., Chulakadabba, A., Russi, M., Ayvazov, S., Benmergui, J., Knapp, M., Kyzivat, E., Miller, C. C., Roche, S., Luo, B., Miller, D. J., Nasr, M., Sun, K., Williams, J. P., MacKay, K., Omara, M., Guanter, L., Gautam, R., Franklin, J., Liu, X., and Wofsy, S. C.: Automatic Methane Plume Masking Based on Wavelet Transform Image Processing: Application to MethaneAIR and MethaneSAT data, EGUsphere, 2026, 1–17, 10.5194/egusphere-2026-141, 2026.